Mohammad Faisal Haider[1]
Department of Mechanical Engineering,
University of South Carolina,
300 Main Street, Room A222,
Columbia, SC 29208
e-mail: haiderm@email.sc.edu

Victor Giurgiutiu
Professor
Fellow ASME
Department of Mechanical Engineering,
University of South Carolina,
300 Main Street, Room A222,
Columbia, SC 29208
e-mail: victorg@sc.edu

Bin Lin
Department of Mechanical Engineering,
University of South Carolina,
300 Main Street, Room A222,
Columbia, SC 29208
e-mail: linbin@cec.sc.edu

Lingyu Yu
Department of Mechanical Engineering,
University of South Carolina,
300 Main Street, Room A222,
Columbia, SC 29208
e-mail: yu3@cec.sc.edu

Poh-Sang Lam
Savannah River National Laboratory,
Aiken, SC 29808
e-mail: ps.lam@srnl.doe.gov

Christopher Verst
Savannah River National Laboratory,
Aiken, SC 29808
e-mail: Christopher.Verst@srs.gov

Effects of Gamma Radiation on Resonant and Antiresonant Characteristics of Piezoelectric Wafer Active Sensors

This paper presents gamma radiation effects on resonant and antiresonant characteristics of piezoelectric wafer active sensors (PWAS) for structural health monitoring (SHM) applications to nuclear-spent fuel storage facilities. The irradiation test was done in a Co-60 gamma irradiator. Lead zirconate titanate (PZT) and Gallium Orthophosphate ($GaPO_4$) PWAS transducers were exposed to 225 kGy gamma radiation dose. First, 2 kGy of total radiation dose was achieved with slower radiation rate at 0.1 kGy/h for 20; h then the remaining radiation dose was achieved with accelerated radiation rate at 1.233 kGy/h for 192 h. The total cumulative radiation dose of 225 kGy is equivalent to 256 years of operation in nuclear-spent fuel storage facilities. Electro-mechanical impedance and admittance (EMIA) signatures were measured after each gamma radiation exposure. Radiation-dependent logarithmic sensitivity of PZT-PWAS in-plane and thickness modes resonance frequency $(\partial(f^R)/\partial(\log_e R_d))$ was estimated as 0.244 kHz and 7.44 kHz, respectively; the logarithmic sensitivity of $GaPO_4$-PWAS in-plane and thickness modes resonance frequency was estimated as 0.0629 kHz and 2.454 kHz, respectively. Therefore, $GaPO_4$-PWAS EMIA spectra show more gamma radiation endurance than PZT-PWAS. Scanning electron microscope (SEM) and X-ray diffraction method (XRD) was used to investigate the microstructure and crystal structure of PWAS transducers. From SEM and XRD results, it can be inferred that there is no significant variation in the morphology, the crystal structure, and grain size before and after the irradiation exposure. [DOI: 10.1115/1.4041068]

Keywords: piezoelectric wafer active sensor, structural health monitoring, electro-mechanical impedance/admittance, gamma radiation effect, PZT, $GaPO_4$, ISFSI

1 Introduction

There is considerable demand for structural health monitoring (SHM) at locations where there are substantial radiation fields. For example, one of the major parts of a nuclear power plant is dedicated to the removal and disposal of spent fuel rod assemblies. In the past, reactors were built to store spent fuel rods in a storage pond for a period ranging from 3 to 5 years. The period of storage is determined either by the need for the fuel to lose most of its radioactivity or the availability of a permanent disposal site. However, since 1977, on-site irradiated fuel storage facilities have been built for storing these irradiated fuel assemblies to prevent the forced shutdown of these plants due to the overflowed of storage pools [1]. The dry cask storage system (DCSS) is such storage facility, which is licensed for temporary storage for nuclear-spent fuel at the independent spent fuel storage installations (ISFSIs) predetermined period. Casks come in different sizes [2]. They are tall enough to hold spent fuel, which can be 14 feet long, and they can weigh up to 150 tons. As of December 2014, just over 2000 casks have been loaded and are safely storing nearly 84,000 spent fuel rod assemblies [2]. Gamma radiation is the major nuclear radiation source near the DCSS. The radioactivity from the canister is about 10 rems per hour (0.1 Gy/h) and outside of the shielding is 25 millirems per year [1]. On Aug. 26, 2014, Nuclear Regulatory Commission (NRC) approved 60 years short-term onsite storage and 100 years long-term storage of spent fuel on site [1,2]. However, steel canisters may start developing corrosion crack within 60 years due to favorable moderate irradiation exposure. It is important to inspect where canisters are cracking or how deep is the existing crack. Regular inspection and tests on cask components are essential for providing safe storage after years. Therefore, it is important to develop an SHM method for DCSS long time evaluation and damage assessment. Permanently installed sensors should provide state of the structure at any time over the entire service life, which is advantageous over traditional ultrasonic nondestructive evaluation techniques. DCSS is a critical safety facility in a nuclear power plant, and it needs of monitoring over prolonged service periods. One of the major goals is to improve DCSS reliability, sustain the safety, and extend the life. Therefore, it is important to develop proper SHM technologies that can better diagnose their state of structural health.

The purpose of SHM techniques is to diagnose the state of the structure [3–7]. EMIA-based SHM technique has been used by many researchers for detecting damage in structure [6–8]. EMIA spectra of piezoelectric wafer active sensors (PWAS) change due to the damage in the host structure [7,9]. In order to use PWAS as an SHM transducer in a nuclear environment, radiation influence

[1]Corresponding author.

Manuscript received March 1, 2018; final manuscript received July 31, 2018; published online September 17, 2018. Assoc. Editor: Kara Peters.

on transducer must be investigated to assure the reliability of the PWAS EMIA method. Any change in the piezoelectric material properties of PWAS can be assessed by observing the change in EMIA spectra.

Piezoelectric wafer active sensors transducers made with piezoelectric material lead zirconate titanate ($PbZrO_3TiO_3$ or PZT), and gallium orthophosphate ($GaPO_4$) were investigated in this research. PZTs exhibit large electromechanical coupling coefficients and piezoelectric constants [10,11]. For PZT-PWAS, APC 850 (APC International, Ltd., Mackeyville, PA) type transducers were used in this research.[2] PZT-PWAS transducer circular in shape with 7 mm diameter. The wafer has a PZT thick film with Ag electrodes on both sides. The thickness of the PZT-PWAS transducer is 0.2 mm. The $GaPO_4$ material is quartz type (α-quartz), which belongs to the class of compounds M–X–O_4. Several researchers [12,13] have investigated $GaPO_4$ as piezoelectric materials. The $GaPO_4$ possess a low piezoelectric constant and low dielectric constant compared to PZT. But compared with quartz crystal, it possesses nearly all the advantages of quartz with higher electromechanical coupling and has thermally stable physical properties up to 950 °C [14–16]. Furthermore, it displays no pyroelectric effect. This article also presents the potential impact on EMIA signature and material degradation of $GaPO_4$ as a piezoelectric material after exposure to Co-60 gamma radiation. Characterization of $GaPO_4$-PWAS after exposure to nuclear radiation has not been yet reported anywhere else. Commercially available high-quality $GaPO_4$-PWAS (PIEZOCRYST GMBH, Graz, Austria)[3] was used in this research. The wafers were x-cut $GaPO_4$ single crystal disks of 7 mm diameter and 0.2 mm thickness. The wafer has a $GaPO_4$ single crystal thick film with Pt electrodes on both sides.

When PWAS transducers work in the subject DCSS environment, radiation may cause degradation or even complete failure of the sensors depending on the sensitivity of the transducers to radiation. Gamma radiation is considered as one of the major radiation sources near the DCSS [17]. In physics, radiation is the emission or transmission of energy in the form of waves or particles through space or a material medium. There are two types of radiation: ionizing (more than 10 eV) and nonionizing [18–20]. A common source of ionizing radiation is radioactive materials that emit α, β, or γ radiation. Gamma radiation consists gamma ray (γ), which is extremely high-frequency electromagnetic radiation and therefore consists of high-energy photons. The measurement unit for gamma radiation dose is the gray, equal to 1 J of absorbed energy per kg of material. The damage caused by gamma rays to PWAS sensors is dependent on the total accumulated dose. The major mechanisms for piezo material performance degradation via gamma-ray interaction are: pinning of the domain, an internal defect due to accumulated ionizing radiation, and radiation-induced charges can be trapped near the electrodes. Such concentration of charge could potentially affect polarizability [20,21]. Pinning of domains may be defined as restricted domain configuration in an unfavorable position. The dipole moment of PWAS transducer material may be changed due to change in the domain configuration after radiation exposure. Sinclair and Chertov conducted a comprehensive literature study in a review paper [22]. In that paper, effects of gamma radiation on piezoelectric properties for several candidate materials were presented. Reliable operation was found of PZT after doses of 1.5 MGy. Ionization damage threshold is 400 MGy of gamma, but only if temperature and neutron fluence are kept low. Signal amplitude decrease is 13% after dose of 22.7 MGy in a customized transducer assembly; drop is believed to be due to a change in piezoelectric efficiency. Parks and Tittmann [23] reported Radiation tolerance of piezoelectric bulk single-crystal aluminum nitride. Kulikov and Yu Trushin [24] conducted a theoretical study of ferroelectric properties degradation in perovskite ferroelectrics and antiferroelectric under neutron irradiation. Giurgiutiu et al. [25] studied radiation, temperature, and vacuum effects on PWAS for space vehicle applications. A small change in resonance and antiresonance frequencies and amplitudes were observed due to radiation, temperature, and vacuum exposure.

In this paper, an experimental investigation was conducted on the gamma irradiation endurance of piezoelectric sensors. PWAS were exposed to cumulative of 225 kGy gamma irradiation. EMIA signature was evaluated before and after the radiation test. Scanning electron microscope (SEM) and X-ray diffraction method (XRD) method was used to investigate PWAS transducer material microstructurally and crystallographically.

1.1 Scope of This Paper. For using PWAS as an SHM transducer in nuclear applications, it is important to investigate the effect of gamma radiation on PWAS transducers. PWAS were exposed to gamma irradiation in two steps: (a) slow irradiation test: 0.1 kGy/h rate for 20 h (b) accelerated irradiation test: 1.233 kGy/h for 192 h. The total accumulated dose for slow radiation and accelerated radiation tests are 2 kGy and 223 kGy, respectively; therefore, in combined total gamma radiation is 225 kGy. Total expected cumulative radiation dose near the DCSS is 876 Gy per year (radiation rate: 0.1 Gy/h). Total cumulative radiation is equivalent to 256 years of total application dose, which is higher than the expected life of DCSS. Slow irradiation test provides an initial assessment of PWAS performance. EMIA and electrical capacitance were measured before and after each slow radiation test. After the preliminary assessment, an equivalent of longtime radiation exposure of PWAS transducers was done for proper SHM applications in the nuclear environment. High doses of gamma radiation from Co-60 and can achieve ionization in a few days that would take years in DCSS applications. PWAS material properties degradation caused by gamma radiation of PWAS is dependent only on the total accumulated dose rather than dose rate if the temperature is kept at constant. Therefore, an accelerated radiation test was conducted in order to achieve equivalent practical dose for prolonged radiation exposure. EMIA and electrical capacitance were measured after each accelerated radiation exposure. PWAS transducer microstructure and crystal structure were investigated before irradiation exposure, after slow radiation exposure, and after accelerated radiation exposure.

2 Theory

Figure 1(*a*) shows radially vibrating PWAS transducer under electric excitation and Fig. 1(*b*) shows the thickness vibrating PWAS transducer under electric excitation. The electromechanical coupling relations of a radially vibrating circular PWAS transducer can be shown as follow [26]:

$$\text{admittance}: \ \overline{Y}(\omega) = i\omega\overline{C}\left[1 - \overline{k}_p^2\left(1 - \frac{(1+\upsilon)J_1(\overline{z})}{\overline{z}J_0(\overline{z}) - (1-\upsilon)J_1(\overline{z})}\right)\right] \tag{1}$$

where $\overline{k}_p = (2/(1-\nu))(d_{31}^2/\overline{s}_{11}^E\overline{\varepsilon}_{33}^T)$; $\overline{C} = \overline{\varepsilon}_{33}^T(\pi a^2/t_a)$; $\overline{z} = (\omega a/\overline{c}_p)$; $\overline{c}_p = \sqrt{(1/\rho\overline{s}_{11}^E(1-\upsilon^2))}$.

$\overline{\varepsilon}_{33}^T$ is the electrical permittivity in the thickness direction; a is the radius of the PWAS transducer; t_a is the thickness of the PWAS transducer; ρ is the density of the PWAS transducer; $\overline{k}_p$ is the in-plane piezoelectric coupling coefficient; $\overline{s}_{11}$ is the complex compliance coefficient; υ is the Poisson's ratio; $J_0(\overline{z})$ and $J_1(\overline{z})$ are the Bessel functions of order 0 and 1; ω is the angular frequency.

Complex compliance and dielectric constant are defined as

$$\overline{s}_{11}^E = s_{11}^E(1 - i\eta) \tag{2}$$

$$\overline{\varepsilon}_{33}^E = \varepsilon_{33}^E(1 - i\delta) \tag{3}$$

where η and δ are dielectric and mechanical loss factor, respectively.

[2] http://www.americanpiezo.com
[3] http://piezocryst.com

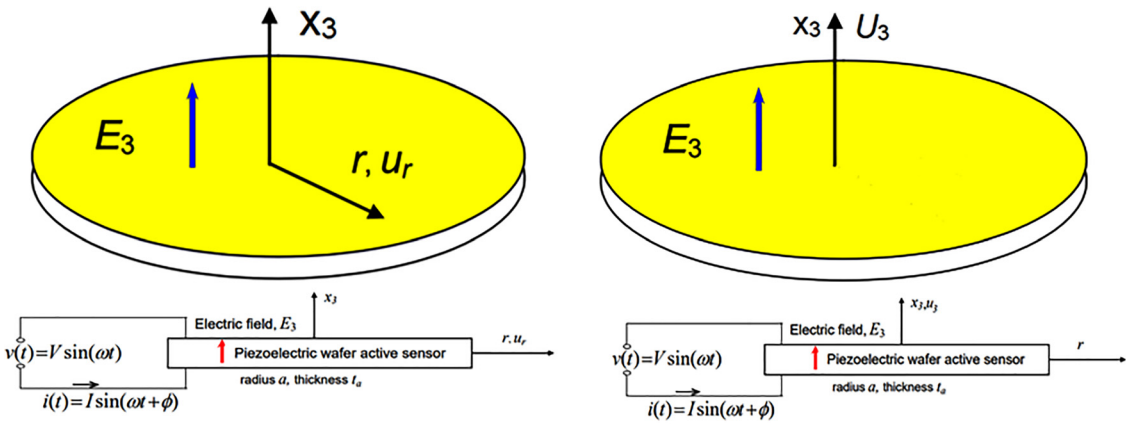

Fig. 1 Simple electro-mechanical system of PWAS under electric excitation (*a*) in-plane vibration and (*b*) thickness vibration [3]

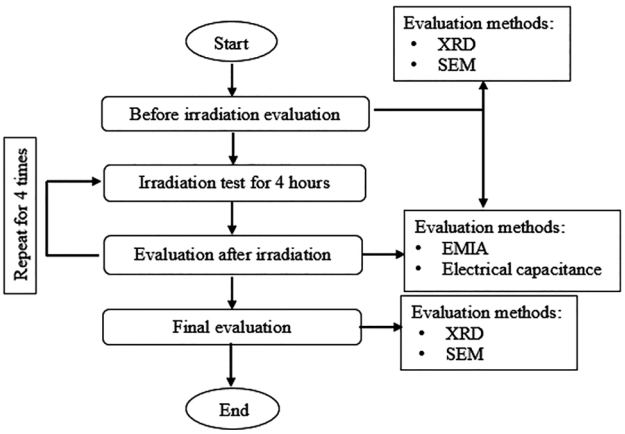

Fig. 2 Experimental procedure flowchart for slow radiation test at 0.1 kGy/h

The coupled relation between the mechanical impedance and complex electrical impedance/admittance for a thickness vibrating circular PWAS transducer can be shown as follows [3]:

$$\text{admittance}: Y = i\omega\overline{C}^{*}\left[1 - \kappa_t^2 \frac{1}{\phi_t \cot\phi_t}\right]^{-1} \tag{4}$$

where $\overline{C}^{*} = \overline{\varepsilon}_{33}^{T}(\pi a^2/t_a)$; $\phi_t = (1/2)(\omega t_a/\overline{c}_t)$; $\overline{c}_t = \sqrt{\overline{c}_{33}^{D}/\rho}$; $\overline{k}_t$ is thickness piezoelectric coupling coefficient.

Complex stiffness can be expressed as

$$\overline{c}_{33}^{D} = c_{33}^{D}(1 - i\eta) \tag{5}$$

3 Experiments of Piezoelectric Wafer Active Sensors Transducer

This section presents details the experimental procedure for evaluating PWAS performance after exposure to (a) slow irradiation test (b) accelerated irradiation test.

3.1 Slow Irradiation Test. For slow radiation experimental study, radiation dose was set to 0.1 kGy/h for 20 h (Cumulative dose: 2 kGy). PWAS were exposed to the radiation for 5 times with 4 h for each time. A set of ten (numbered from 1 to 10) nominally identical free PWAS (PZT and $GaPO_4$) were tested. The irradiation test was done in a Co-60 gamma irradiator facility (by J. L. Shepherd and Associates). The experimental procedure is shown in Fig. 2.

3.1.1 Accelerated Irradiation Test. For accelerated radiation experiment study, radiation dose was set at 1.233 kGy/h for 192 h (Cumulative dose: 223 kGy). Radiation dose analysis is shown in Table 1. Last 80 h radiation test was done only to a subset (four samples from each group). In order to determine the stability of PWAS transducers under gamma radiation, the following experimental procedure was followed.

Step 1: Transducers were exposed to gamma radiation at 1.233 kGy/h continuously for 16 h

Table 1 Radiation dose analysis for DCSS applications

Radiation rate	Radiation exposure time (h)	Radiation exposure (kGy/h)	Accumulated exposure time (kGy)	Accumulated radiation (kGy)	Equivalent to application dose (years)
Slow radiation test					
0.1	4	0.4	4	0.4	0.45
	4	0.4	8	0.8	0.9
	4	0.4	12	1.2	1.4
	4	0.4	16	1.6	1.82
	4	0.4	20	2.0	2.28
Accelerated radiation test					
1.23	16	19.7	36	21.7	24.7
	16	19.1	52	40.8	46.6
	80	92.7	132	133.5	152.4
	80	92.0	212	225	256

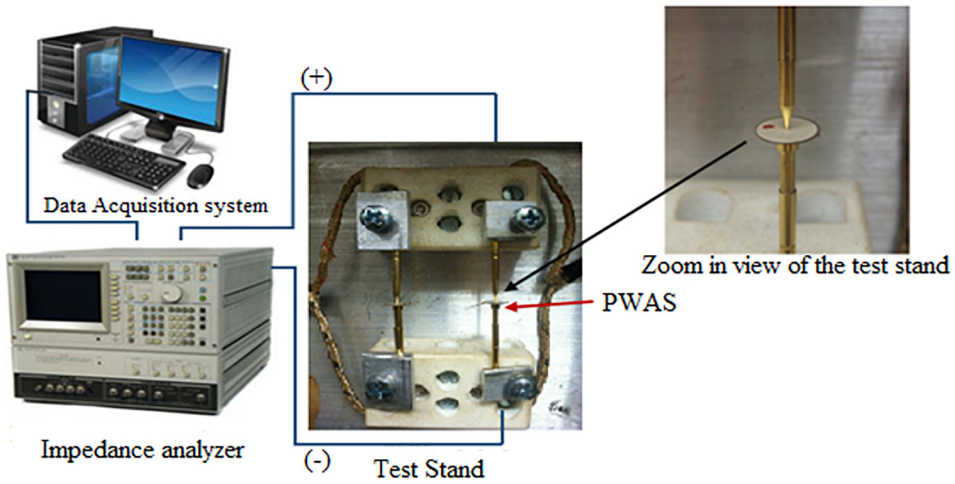

Fig. 3 Experimental setup for EMIA measurement using impedance analyzer

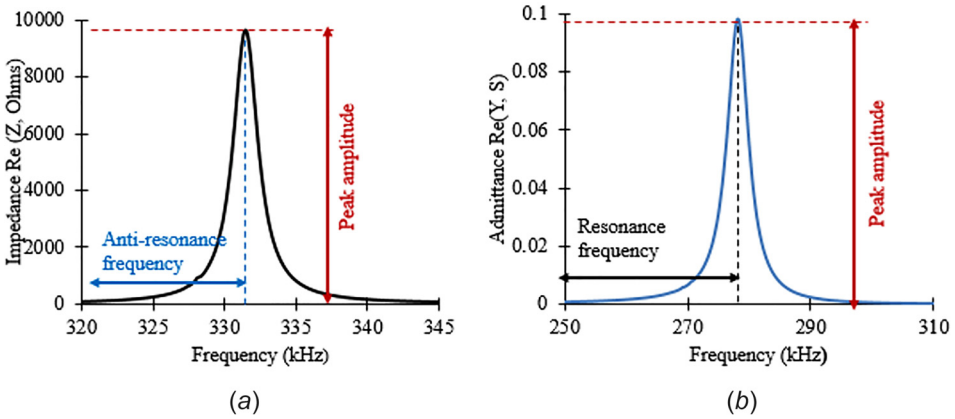

Fig. 4 Typical EMIA spectra of a circular PWAS: (*a*) impedance spectra (antiresonance phenomenon) (*b*) admittance spectra (resonance phenomenon)

Step 2: EMIA and electrical capacitance were measured
Step 3: Repeat step 1 and step 2 for additional 176 h with 16 h, 80 h, and 80 h exposure
Step 6: Final evaluation:

- EMIA and electrical capacitance were measured
- SEM system was used to visualize the cross section of PWAS transducer
- XRD spectrum was used to identify a change in crystal structure, unit cell dimension, and symmetry

3.2 Electro-Mechanical Impedance and Admittance Measurement. Electro-mechanical impedance and admittance and electrical capacitance of a set of nominally identical free PWAS transducers were measured in each step. Figure 3 shows the experimental setup for EMIA measurement [27]. For PZT, the EMIA were collected from 250 kHz to 350 kHz with a step size of 50 Hz during in plane mode and 10 MHz to 13 MHz with a step size of 250 Hz during thickness mode measurement. For $GaPO_4$, the EMIA were collected from 270 kHz to 300 kHz with a step size of 1 Hz during in plane mode and 8 MHz to 11 MHz with a step size of 250 Hz during thickness mode measurement. The real part of the EMIA is used in this research [28–30]. First PWAS antiresonance and resonance was considered in this paper as it shows more stable response than higher resonance or antiresonance spectrum [31].

The capacitance of the transducer can be measured by using following formula:

$$\overline{C} = \bar{\varepsilon}\frac{A}{d} \tag{6}$$

Here, $\bar{\varepsilon} = \varepsilon' - i\varepsilon'' = (-i/\omega Z^*(\omega)C_0)$ and $C_0 = (\varepsilon_0 A/d)$; $\varepsilon_0 = 8.85 \times 10^{-12}$ F/m; A is the area of the sample and d is the thickness of the sample.

The measured impedance of the transducer is $Z^* = Z' + iZ''$. Here, Z' is the real part and Z'' is the imaginary part of the impedance.

4 Results and Discussion

4.1 Electro-Mechanical Impedance and Admittance of Lead Zirconate Titanate-Piezoelectric Wafer Active Sensors Transducers. Figure 4 shows the typical EMIA spectra of a circular PWAS. Antiresonance frequency is the frequency at which the impedance spectral peak is observed, and the corresponding value of the peak is the antiresonance amplitude. Similarly, the resonance frequency is the frequency at which the admittance spectral peak is observed, and the corresponding value of the peak is the antiresonance amplitude.

Change in the resonance/antiresonance frequency and amplitude are the key factors for evaluating PWAS transducer piezoelectric performance. The major mechanisms for piezoelectric material properties degradation via gamma-ray interaction are considered as follows:

(1) The primary degradation mechanism is pinning of domain
(2) Accumulated exposure to ionizing radiation can cause an internal defect

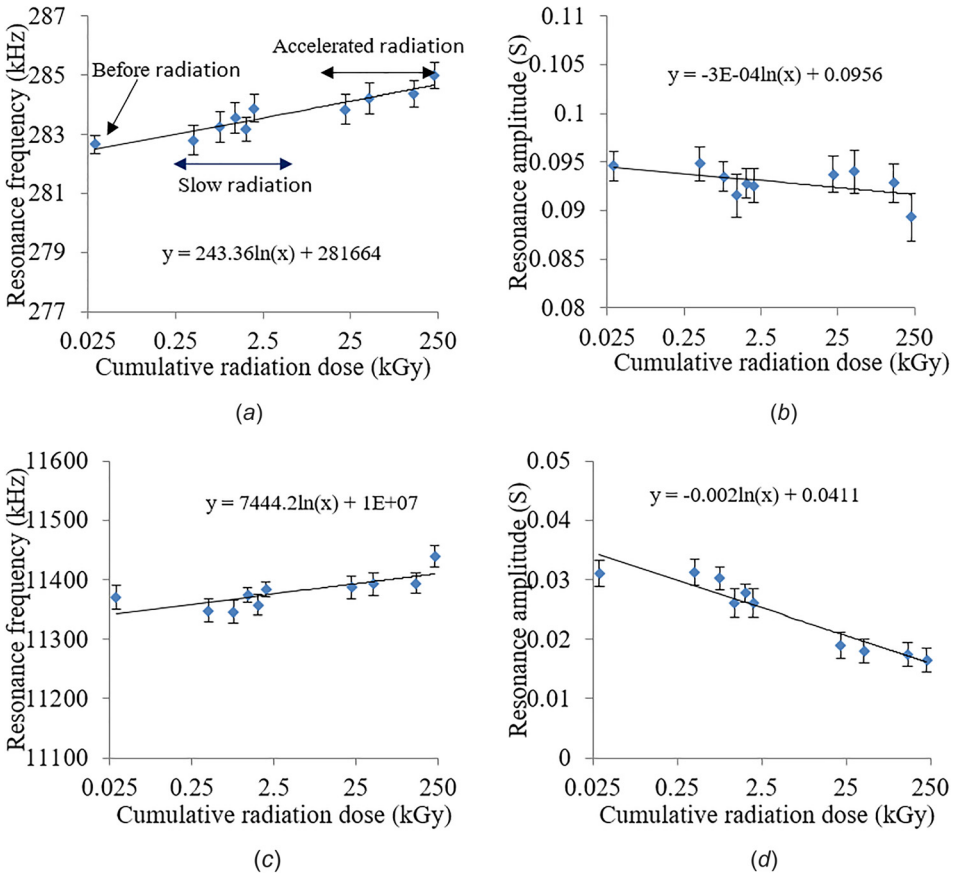

Fig. 5 ((*a*) and (*b*)) Resonance frequency and amplitude for radially vibrating PZT-PWAS; ((*c*) and (*d*)) resonance frequency and amplitude for thickness vibrating PZT-PWAS, with cumulative gamma radiation dose

(3) Radiation-induced charges can be trapped near the electrodes. Such concentration of charge could potentially affect polarizability.

Figures 5(*a*)–5(*d*) show the change of resonance frequency and amplitude for both radially and thickness vibrating PZT-PWAS transducers with accumulated gamma radiation. To facilitate the understanding of the plot of PWAS EMIA with exposed radiation, slow radiation part and accelerated radiation part of the total dose are shown in Fig. 5(*a*). Rest of the figures carries the same information as Fig. 5(*a*). In order to respond to skewness toward large radiation dose, the cumulative radiation dose values are plotted in log scale (*x*-axis). A small radiation exposure (∼30 Gy) was assigned to the before radiation test data in order to plot in the log scale.

Figures 5(*a*) and 5(*c*) show the change in resonance frequency with accumulated radiation dose for in-place and thickness vibrating PZT-PWAS, respectively, whereas Figs. 5(*b*) and 5(*d*) show the change in resonance amplitude with accumulated radiation dose for in-place and thickness vibrating PZT-PWAS, respectively. The mean resonance frequency before the radiation of radially and thickness vibrating PWAS are 287 kHz and 1134 kHz, respectively. The error bar is obtained from the data of six identical PWAS. The resonance frequency (Figs. 5(*a*) and 5(*c*)) increases at the higher rate initially but at higher cumulative radiation dose the frequency increases at a slower rate. Therefore, the resonance frequency follows a logarithmic increment with radiation dose. The resonance amplitude shows the opposite phenomenon i.e., resonance amplitude decreases logarithmically with radiation dose.

However, the change in resonance frequency for thickness vibrating PZT-PWAS is significant compared to radially vibrating PZT-PWAS. Equations (1) and (5) show that amplitude of impedance and admittance value depend on capacitance and piezoelectric coupling factor. Piezoelectric coupling depends on piezoelectric constant and capacitance. Therefore, resonance amplitude decreases due to the change in capacitance and

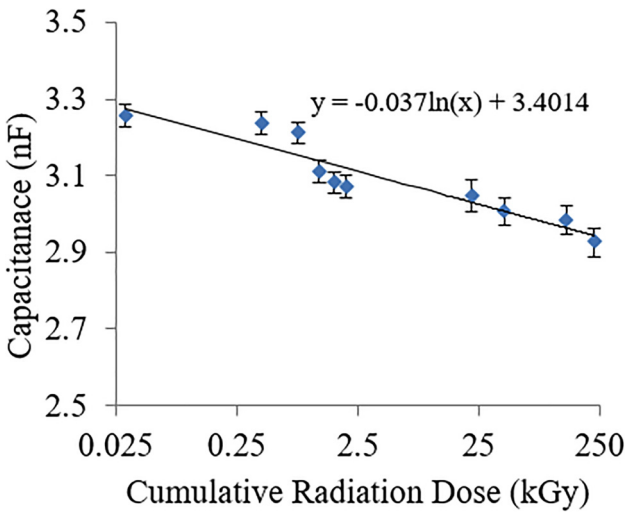

Fig. 6 Electrical capacitance (measured at 1 kHz) of PZT-PWAS with cumulative radiation dose

piezoelectric constant of the piezoelectric sensor with increasing radiation dose.

Figure 6 shows the change in electrical capacitance measured at 1 kHz after exposure to different radiation dose. Electrical capacitance decreases logarithmically as radiation absorbed dose increases. Several polarization mechanisms are responsible for changing the dielectric response [32]. Among them, pinning of the domain is the key factor to the change the dielectric response of PZT-PWAS transducer [27,33–37]. Many researchers have reported decreasing capacitance value with increasing radiation dose [38,39].

Pinning of domain affects the piezoelectric coefficient as well as piezoelectric coupling. The piezoelectric effect is a linear coupling between the polarization and the applied stress field. Radiation exposure of the piezoelectric materials may restrict the domain in an unfavorable position, hence leading to degraded net polarization. Therefore, piezoelectric coupling factor decreases as radiation exposure increases. The temperature may have also effect on dielectric properties of the PWAS transducers. Therefore, the temperature was monitored periodically during the radiation exposure test. Only 1–2 °C temperature fluctuation from room temperature was observed.

Figures 7(*a*)–7(*d*) show the change of antiresonance frequency and amplitude for both radially and thickness vibrating PZT-PWAS transducers with accumulated gamma radiation. Figure 7 shows that both antiresonance frequency and the amplitude increase logarithmically with increasing radiation dose. The antiresonance (Eqs. (1) and (5)) amplitude is inversely proportional to the capacitance. Antiresonance value also depends on piezoelectric coupling [39]. Therefore, decreasing capacitance and piezoelectric coupling value in combination resulting increasing of antiresonance amplitude. Antiresonance frequency shows larger variation than resonance frequency with applied radiation dose. Resonance frequency depends on poison's ratio, density, stiffness, and mechanical loss factor [27]. The extrinsic contribution of the domain may contribute to change stiffness and mechanical loss factor resulting in a change in resonance frequency. However, antiresonance frequency depends on poison's ratio, density, stiffness, piezoelectric coupling factor, electrical capacitance, mechanical loss factor, and dielectric loss [27]. The change in piezoelectric coupling factor, electrical capacitance, mechanical loss factor, and dielectric loss contributes a larger change in antiresonance frequency. In addition, the mechanical loss factor also contributes to the change in resonance frequency and amplitude. During the resonance, the transducer goes through mechanical friction and contributed to more dissipation loss. During antiresonance, the transducer moves hardly resulting in very little mechanical friction, and thus it showed a very low mechanical loss. This mechanical loss changes with changing domain configuration due to radiation effect. A future analytical study would be recommended for understanding the PWAS transducers properties with radiation dose.

4.2 Electro-Mechanical Impedance and Admittance of $GaPO_4$-Piezoelectric Wafer Active Sensors Transducers. Figures 8(*a*) and 8(*c*) show the change of resonance frequency with radiation for in-plane and thickness modes, respectively. The

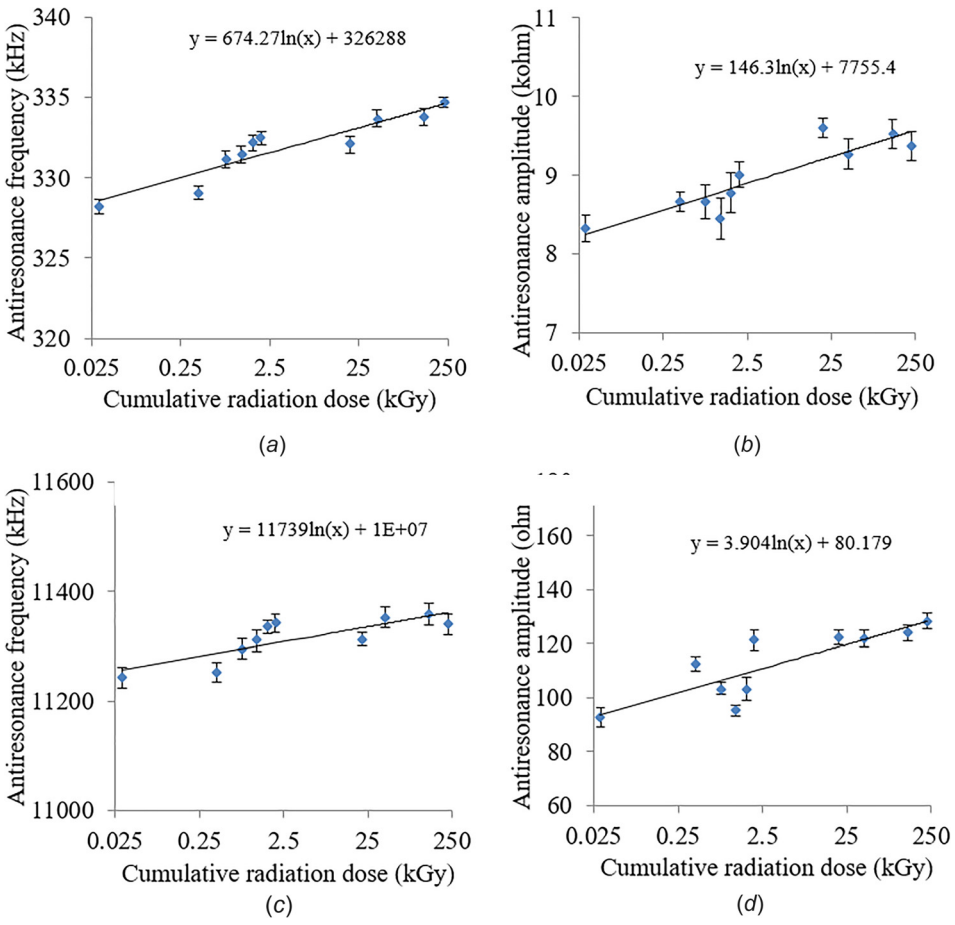

Fig. 7 ((*a*) and (*b*)) Antiresonance frequency and amplitude for radially vibrating PZT-PWAS; ((*c*) and (*d*)) antiresonance frequency and amplitude for thickness vibrating PZT-PWAS, with cumulative gamma radiation dose

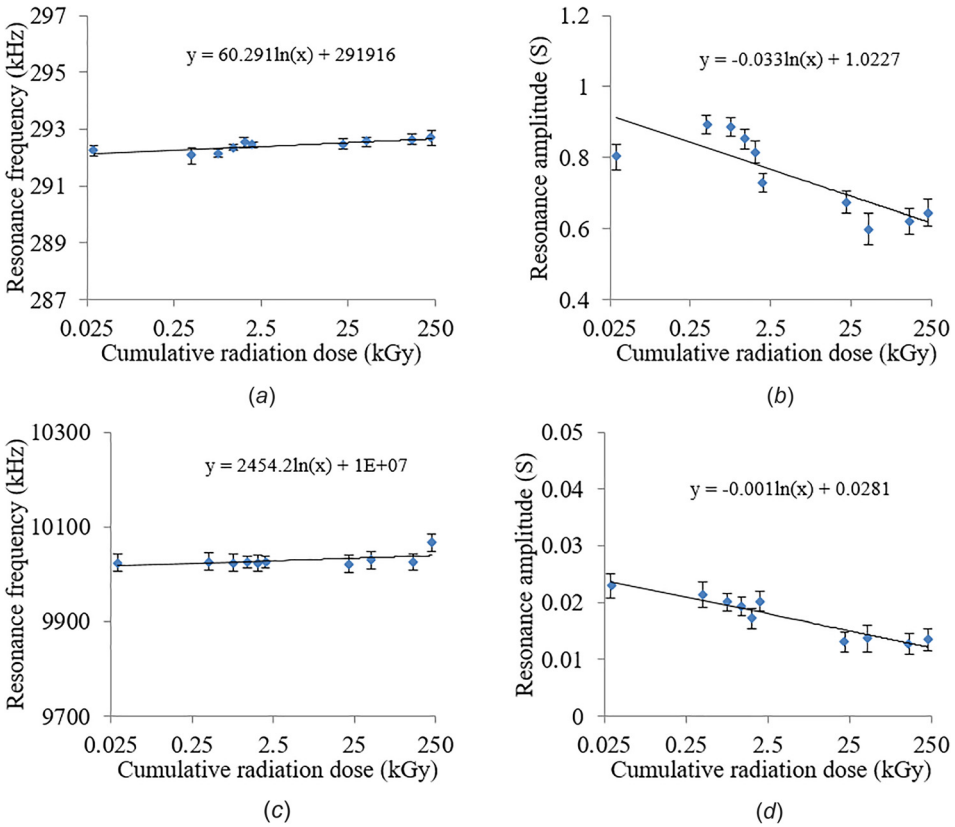

Fig. 8 ((*a*) and (*b*)) Resonance frequency and amplitude for radially vibrating $GaPO_4$ PWAS; ((*c*) and (*d*)) resonance frequency and amplitude for thickness vibrating $GaPO_4$ PWAS, with cumulative gamma radiation dose

resonance frequency increases slightly with increasing exposed radiation dose whereas, the resonance amplitude decreases with increasing exposed radiation dose. However, large scatter of resonance amplitude between the samples resulted in a large standard error (error bar). Due to the high electrical resistivity of $GaPO_4$-PWAS, it shows very low resonance amplitude (Fig. 8(*b*)). The change in resonance frequency and amplitude can be explained by the role of Ga–O–P interactions [40–42].

The Ga–O and P–O distances may contract due to radiation exposure, based on the ionic radii it may change Ga–O–P angle. The change in Ga–O–P angle may contribute to change in capacitance and piezoelectric performance as well as mechanical and electrical loss. Figure 9 shows the change in electrical capacitance of $GaPO_4$-PWAS with cumulative radiation dose. The capacitance value decreases with increasing radiation dose. The resonance amplitude is proportional to capacitance; therefore, decreasing resonance amplitude with increasing radiation dose is expected.

Figure 10 shows the change in antiresonance frequency and amplitude with exposed radiation dose. For both radially vibrating and thickness vibrating $GaPO_4$-PWAS, the resonance frequency increases logarithmically (Figs. 10(*a*) and 10(*c*)) with increasing radiation dose. Decreasing electrical capacitance value and piezoelectric coupling results in an increase of antiresonance amplitude (Figs. 10(*c*) and 10(*d*)). The antiresonance frequency shows larger variation than the resonance frequency. Dielectric and mechanical loss due to change in Ga–O–P angle may contribute to the larger variation in antiresonance frequency.

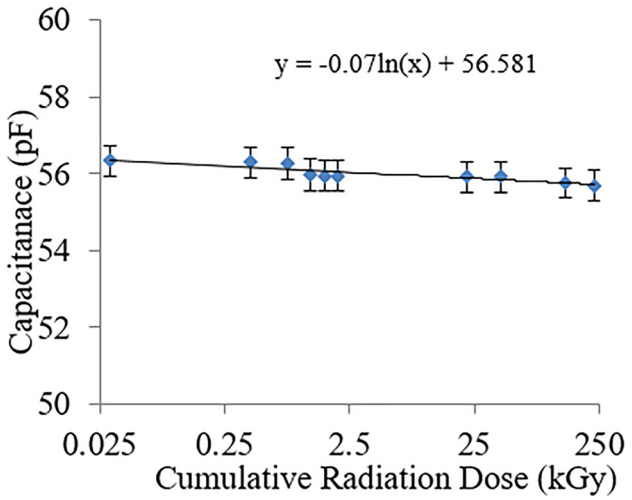

Fig. 9 Electrical capacitance (measured at 1 kHz) of $GaPO_4$-PWAS with cumulative radiation dose

4.3 Microstructural and Crystallographic Investigation. This section investigates the microstructure and crystal structure of the PWAS transducers. The microstructure of the PWAS was examined using SEM where crystal structure was investigated by XRD method. SEM and XRD examinations were performed at different stages: before exposure to radiation, after slow radiation test, and after accelerated radiation test. SEM images of PWAS transducers (Ag/PZT/Ag and Pt/$GaPO_4$/Pt) cross section before and after exposure to gamma radiation are shown in Figs. 11 and 12 PZT-PWAS transducer has two Ag electrodes on top and

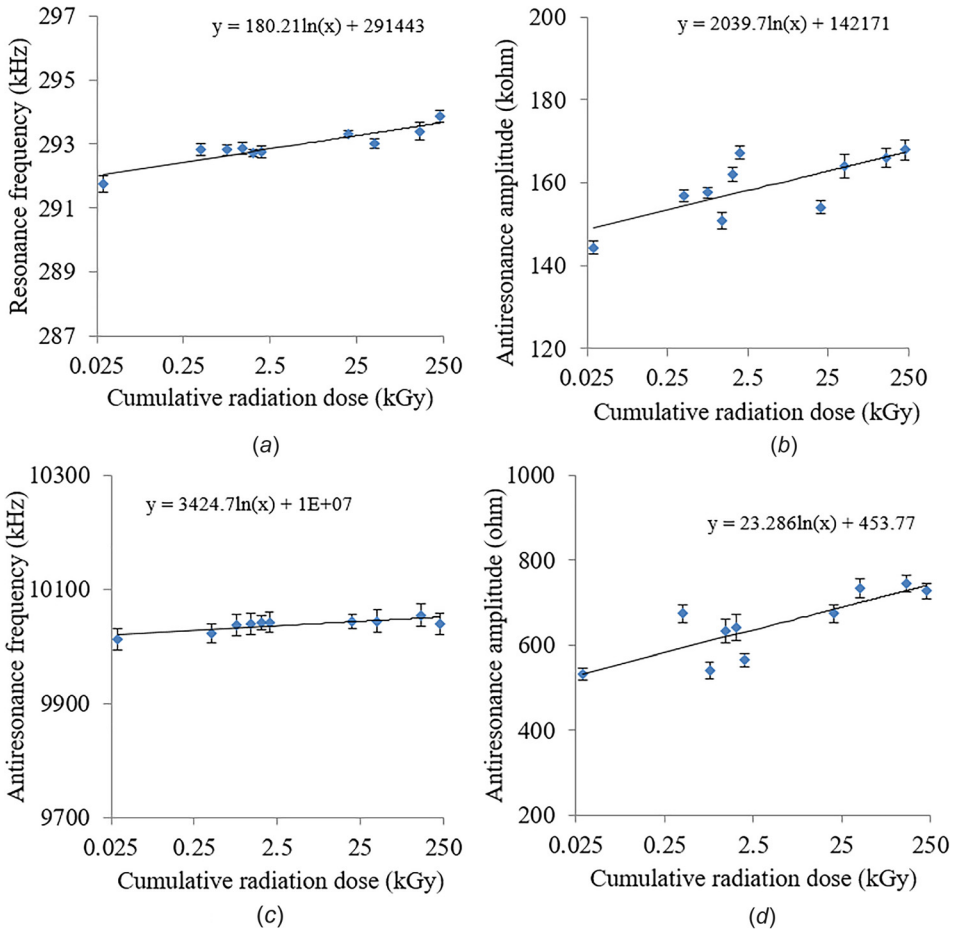

Fig. 10 ((*a*) and (*b*)) Antiresonance frequency and amplitude for radially vibrating $GaPO_4$ PWAS; ((*c*) and (*d*)) antiresonance frequency and amplitude for thickness vibrating $GaPO_4$ PWAS, with cumulative gamma radiation dose

bottom with multidomain PZT in between them (Fig. 11). $GaPO_4$ also has two Pt electrodes on top and bottom with single crystal $GaPO_4$ in between them (Fig. 12). No significant variation was found in the microstructure (PZT grains and $GaPO_4$ single crystal) PWAS transducers due to radiation exposure (Figs. 11 and 12). As there was no significant change in the microstructure, only SEM images before and after gamma radiation exposure are reported in this paper. A future study would be recommended to examine the domain configuration of PZT by transmission electron microscopy. However, to observe the change in the domain, an in situ radiation experiment would be needed. Other defects such as accumulation of charges near the electrode are at the atomic level. A future study would also be recommended to observe the charge accumulation using atomic force microscopy. Figures 13 and 14 show the XRD spectrum for PWAS transducer material. The important feature of the XRD measurement is X-ray diffraction peak with diffraction angle (2θ). Any change in the crystal structure shifts the peak with diffraction angle (2θ). Figure 13 show no significant change in X-ray diffraction peak position of PZT-PWAS transducer material. Figure 14 shows that the overall XRD patterns of $GaPO_4$-PWAS transducer material remain the same before and after radiation exposure. A very small shift in the position of X-ray diffraction peak toward the higher angle side (first large X-ray diffraction peak appears at 26.25 deg and 26.45 deg for unexposed and 225 kGy radiated $GaPO_4$-PWAS, respectively) indicates a slight contraction in the lattice due to radiation-induced effect. SEM and XRD studies confirm that there was no significant variation in PWAS transducer microstructure and crystal structure.

5 Radiation-Dependent Sensitivity of Electro-Mechanical Impedance and Admittance and Electrical Capacitance of Piezoelectric Wafer Active Sensors for Structural Health Monitoring Applications

Piezoelectric wafer active sensors transducers show some changes in EMIA spectra with radiation. In order to use the PWAS transducers in SHM applications, radiation-dependent sensitivity need to be determined and the radiation effect on EMIA reading need to be evaluated. Mean values and standard errors from a set of identical PWAS transducers are plotted from Figs. 5 to 10 The changes in antiresonance and resonance frequency and amplitude as a function of radiation dose are shown in their respective plots. From these figures, it can be inferred that antiresonance amplitude decreases logarithmically with exposed radiation, whereas values of resonance amplitude increase as radiation dose increases. Values of antiresonance and resonance frequencies decrease logarithmically as radiation dose increases. Hence, the following radiation compensation formula can be proposed:

$$f^{\mathrm{R/AR}}(R) = f_o^{\mathrm{R/AR}} + m_f^{\mathrm{R/AR}} \log_e R_d \tag{7}$$

Here, $f^{\mathrm{R/AR}}$ is the resonance/antiresonance frequency; R_d is the accumulated radiation dose; is the slope of the resonance/antiresonance curve; $f_o^{\mathrm{R/AR}}$ is the frequency axis intercept.

The slope of the resonance/antiresonance curve can be written as

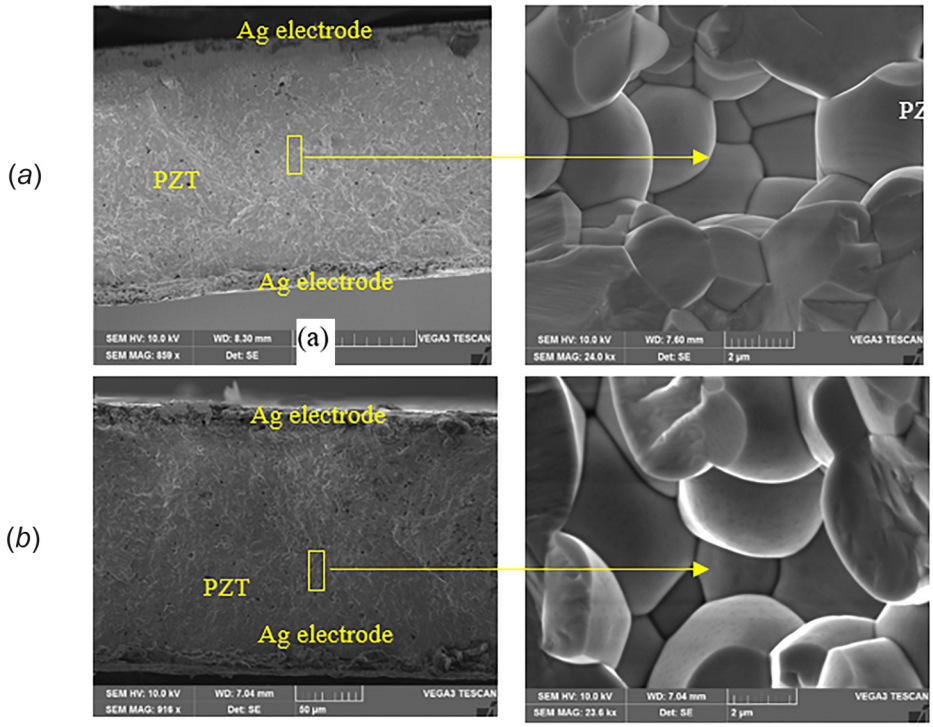

Fig. 11 Scanning electron microscope micrograph of cross section of Ag/PZT/Ag PWAS transducer (*a*) before irradiation and (*b*) after accelerated radiation of 225 kGy

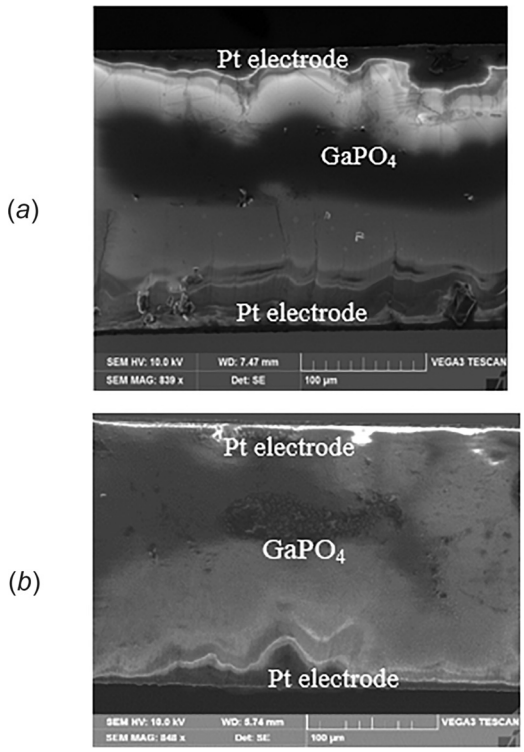

Fig. 12 Scanning electron microscope micrograph of cross section of Pt/$GaPO_4$/Pt PWAS transducer (*a*) before irradiation and (*b*) after accelerated radiation of 225 kGy

$$\frac{\partial\left(f^{\mathrm{R/AR}}\right)}{\partial(\log_e R_d)} = m_f^{\mathrm{R/AR}} \tag{8}$$

Here, $m_f^{\mathrm{R/AR}}$ is defined as the logarithmic sensitivity of Eq. (11). Therefore, change of frequency at particular radiation dose depends on the logarithmic value of radiation dose.

Similarly, for resonance/antiresonance amplitude and electrical capacitance, sensitivity can be defined as

$$\frac{\partial\left(A^{\mathrm{R/AR}}\right)}{\partial(\log_e R_d)} = m_A^{\mathrm{R/AR}} \tag{9}$$

$$\frac{\partial(C)}{\partial(\log_e R_d)} = m_C \tag{10}$$

Here, $A^{\mathrm{R/AR}}$ is the resonance/antiresonance amplitude; C is the electrical capacitance; R_d is the accumulated radiation dose; and m_C is the slope of the amplitude and electrical capacitance curve. The compensation formula can be used based on the accumulated radiation dose in practical applications. The accumulated radiation dose directly related to the service time of a structure in a nuclear environment. If the accumulated radiation dose is known, then the expected change in the resonance/antiresonance frequency and amplitude can be traced back using the compensation formula. That would be beneficial for excluding the irradiation effect from the structurally damaged EMIA signal.

Table 2 shows the instantaneous sensitivity of PWAS resonance/antiresonance frequency, amplitude, and electrical capacitance. Radiation-dependent logarithmic sensitivity of PZT-PWAS in-plane and thickness resonance frequency was estimated as 0.244 kHz and 7.44 kHz, respectively, whereas, the logarithmic sensitivity of PZT-PWAS in-plane and thickness antiresonance frequency is higher 0.674 kHz and 11.7 kHz, respectively. The Similarly, the logarithmic sensitivity of $GaPO_4$-PWAS in-plane and thickness resonance frequency was estimated as 0.0629 kHz and 2.454 kHz, respectively, whereas, the logarithmic sensitivity of $GaPO_4$-PWAS in-plane and thickness antiresonance frequency is higher 0.18 kHz and 3.42 kHz, respectively. Therefore, $GaPO_4$-PWAS EMIA spectra show more gamma radiation endurance than PZT-PWAS. By observing Table 2, it can be inferred that the resonance frequency shows less radiation sensitivity than antiresonance frequency. The same conclusion can be drawn for resonance amplitude over antiresonance amplitude.

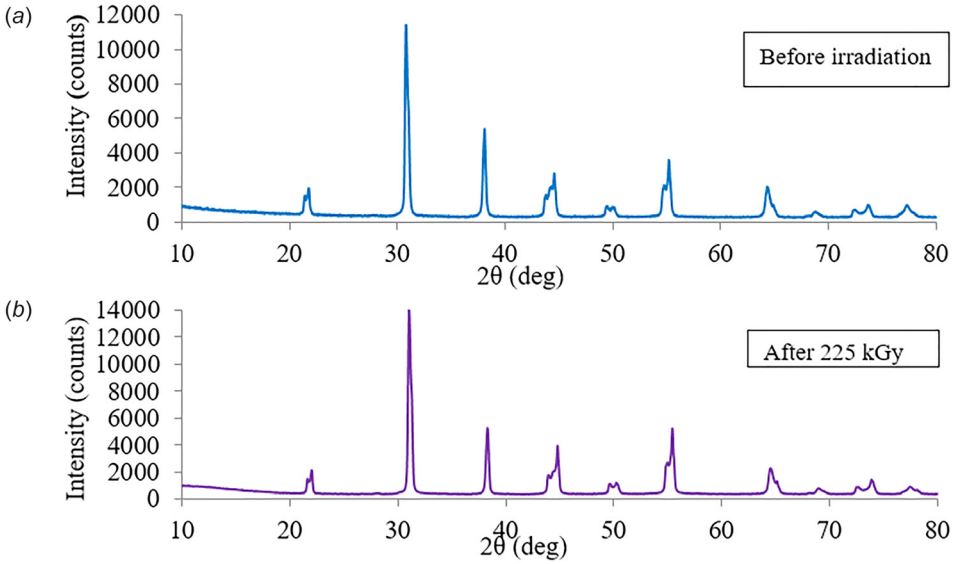

Fig. 13 X-ray diffraction method of PZT-PWAS transducer (*a*) before irradiation and (*b*) after accelerated radiation of 225 kGy

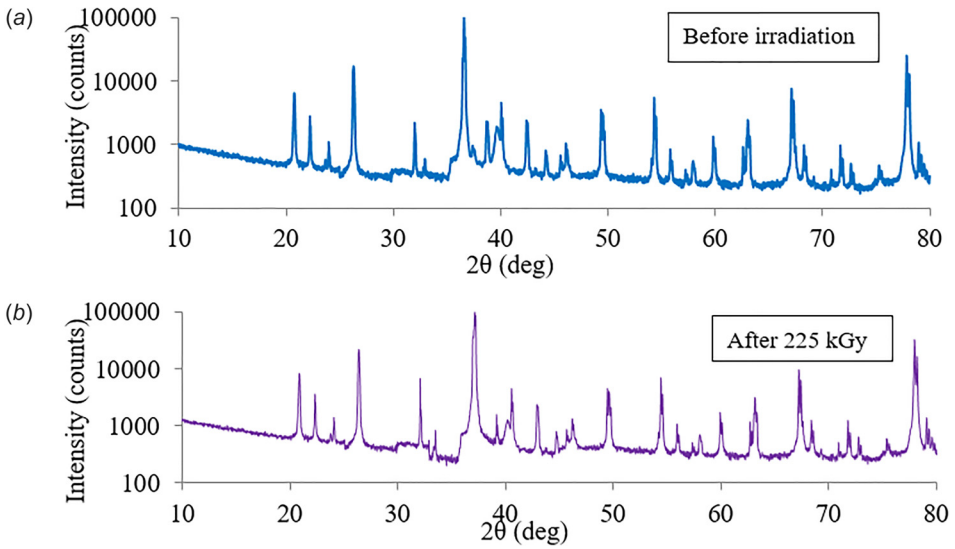

Fig. 14 X-ray diffraction method of $GaPO_4$-PWAS transducer (*a*) before irradiation and (*b*) after accelerated radiation of 225 kGy

Table 2 Gamma radiation effect on EMIA of PWAS transducers

		Sensitivity with radiation $\left(\frac{\partial(f^{R/AR}, A^{R/AR})}{\partial(\log_e R_d)}\right)$				
Direction	PWAS types	Resonance frequency $\frac{\partial(f^A)}{\partial(\log_e R_d)}$(kHz)	Resonance amplitude $\frac{\partial(A^A)}{\partial(\log_e R_d)}$ S	Antiresonance frequency $\frac{\partial(f^{AR})}{\partial(\log_e R_d)}$ (kHz)	Antiresonance amplitude $\frac{\partial(A^{AR})}{\partial(\log_e R_d)}$ ohm	Capacitance $\frac{\partial(C)}{\partial(\log_e R_d)}$
In-plane	PZT	0.244	-3×10^{-4}	0.674	146.3	—
Thickness	PZT	7.44	−0.002	11.7	3.904	−0.037 nF
In-plane	$GaPO_4$	0.0629	−0.033	0.180	2039.7	—
Thickness	$GaPO_4$	2.454	−0.001	3.42	23.28	−0.07 pF

6 Summary and Conclusion

6.1 Summary. To develop proper SHM techniques for DCSS, EMIA response of free PWAS transducers was evaluated after gamma radiation exposure. The PWAS transducers were made of PZT material and $GaPO_4$ crystal. Piezoelectric material degradation of PWAS transducers was observed due to gamma radiation exposure. Values of antiresonance and resonance frequencies decrease logarithmically as radiation dose increases.

The tentative statistical analysis was conducted to find the logarithmic sensitivity of resonance and antiresonance frequencies and amplitudes with radiation. Radiation-dependent logarithmic sensitivity of PZT-PWAS in-plane and thickness resonance frequency $(\partial(f^R)/\partial(\log_e R_d))$ was estimated as 0.244 kHz and 7.44 kHz, respectively, whereas, the logarithmic sensitivity $(\partial(f^R)/\partial(\log_e R_d))$ of $GaPO_4$-PWAS in-plane and thickness resonance frequency was estimated as 0.0629 kHz and 2.454 kHz, respectively.

Scanning electron microscopy and XRD was used to investigate the microstructure and crystal structure of the PWAS transducer material receptively. No significant change in microstructure morphology and crystal structure was observed.

The change in material properties of PZT-PWAS may be explained by the pinning of domain walls by some radiation-induced effect, whereas, material properties degradation behavior of $GaPO_4$-PWAS may be explained by the change in Ga–O; P–O distances and Ga–O–P angle.

6.2 Conclusion. The experiment showed that PWAS transducers might have some sensitivity to gamma radiation. A detailed experiment was conducted to evaluate PWAS performance after gamma radiation. Changes in resonance/antiresonance frequencies and amplitudes in the PWAS transducers were evaluated. For $GaPO_4$-PWAS, slight variation in resonance and antiresonance frequencies of both in-plane and thickness modes was observed, whereas for PZT-PWAS, larger variation in resonance and antiresonance frequencies of both in-plane and thickness modes was observed. Therefore, it can be concluded that $GaPO_4$-PWAS transducers show more radiation endurance than PZT-PWAS. It was found that the changes in resonance and antiresonance frequencies have a logarithmic relationship with radiation dose. This relation could provide radiation compensation in a nuclear environment and could be useful for proper damage detection. Hence, a compensation technique has been proposed to take care of this aspect. This compensation technique could be useful to distinguish irradiation effect from EMIA signal for structural damage detection in nuclear-spent fuel storage facilities.

Acknowledgment

The authors would like to acknowledge the help from The Electron Microscopy Center, USC for the SEM; Chemistry Department, USC for XRD measurements.

Funding Data

- The U.S. Department of Energy (DOE), Office of Nuclear Energy, under Grant Nos. DE-NE 0000726 and DE-NE 0008400.

References

[1] Michele, S., 2015, "Dry Cask Storage-The Basics," Wordpress.com, San Francisco, CA., (epub).

[2] NRC News, 2018, "Dry Cask Storage," Nuclear Regulatory Commission, Washington, DC, accessed Aug. 8, 2018, https://www.nrc.gov/waste/spent-fuel-storage/dry-cask-storage.html

[3] Giurgiutiu, V., 2014, *Structural Health Monitoring With Piezoelectric Wafer Active Sensors*, 2nd ed., Academic, New York.

[4] Haider, M. F., and Giurgiutiu, V., 2018, "A Helmholtz Potential Approach to the Analysis of Guided Wave Generation During Acoustic Emission Events," ASME J. Nondestr. Eval., Diagn. Prognostics Eng. Syst., **1**(2), p. 021002.

[5] Haider, M. F., and Giurgiutiu, V., 2017, "Analysis of Axis Symmetric Circular Crested Elastic Wave Generated During Crack Propagation in a Plate: A Helmholtz Potential Technique," Int. J. Solids Struct., **134**, pp. 130–150.

[6] Zhao, X., Gao, H., Zhang, G., Ayhan, B., Yan, F., Kwan, C., and Rose, J. L., 2007, "Active Health Monitoring of an Aircraft Wing With Embedded Piezoelectric Sensor/Actuator Network: I. Defect Detection, Localization and Growth Monitoring," Smart Mater. Struct., **16**(4), p. 1208.

[7] Ciang, C. C., Lee, J. R., and Bang, H. J., 2008, "Structural Health Monitoring for a Wind Turbine System: A Review of Damage Detection Methods," Meas. Sci. Technol., **19**(12), p. 122001.

[8] Park, G., Farrar, C. R., Rutherford, A. C., and Robertson, A. N., 2006, "Piezoelectric Active Sensor Self-Diagnostics Using Electrical Admittance Measurements," ASME J. Vib. Acoust., **128**(4), pp. 469–476.

[9] Bhalla, S., and Soh, C. K., 2004, "Structural Health Monitoring by Piezo-Impedance Transducers. I: Modeling," J. Aerosp. Eng., **17**(4), pp. 154–165.

[10] Newnham, R. E., Xu, Q. C., Kumar, S., and Cross, L. E., 1990, "Smart Ceramics," Ferroelectrics, **102**(1), pp. 259–266.

[11] Veríssimo, M. I. S., Mantas, P. Q., Senos, A. M. R., Oliveira, J. A. B. P., and Gomes, M. T. S. R., 2003, "Suitability of PZT Ceramics for Mass Sensors Versus Widespread Used Quartz Crystals," Sens. Actuators B: Chem., **95**(1–3), pp. 25–31.

[12] Giurgiutiu, V., Xu, B., and Liu, W., 2010, "Development and Testing of High-Temperature Piezoelectric Wafer Active Sensors for Extreme Environments," Struct. Health Monit., **9**(6), pp. 513–525.

[13] Haines, J., Cambon, O., Prudhomme, N., Fraysse, G., Keen, D. A., Chapon, L. C., and Tucker, M. G., 2006, "High-Temperature, Structural Disorder, Phase Transitions, and Piezoelectric Properties of $GaPO_4$," Phys. Rev. B, **73**(1), p. 014103.

[14] Reiter, C., Krempl, P. W., Thanner, H., Wallnöfer, W., and Worsch, P. M., 2001, " Material Properties of $GaPO_4$ and Their Relevance for Applications," Ann. Chim. Sci. Matér., **26**(1), pp. 91–94.

[15] Philippot, E., Palmier, D., Pintard, M., and Goiffon, A., 1996, "A General Survey of Quartz and Quartz-Like Materials: Packing Distortions, Temperature, and Pressure Effects," J. Solid State Chem., **123**(1), pp. 1–13.

[16] Krempl, P., Schleinzer, G., and Wallno, W., 1997, "Gallium Phosphate, $GaPO_4$: A New Piezoelectric Crystal Material for High-Temperature Sensorics," Sens. Actuators A: Phys., **61**(1–3), pp. 361–363.

[17] Sindelar, R. L., Duncan, A. J., Dupont, M. E., Lam, P.-S., Louthan, M. R., Jr., and Skidmore, T. E., 2011, "Materials Aging Issues and Aging Management for Extended Storage and Transportation of Spent Nuclear Fuel," Office of Nuclear Reactor Regulation, U.S. Nuclear Regulatory Commission, Washington, DC, Report No. NUREG/CR-7116 (SRNL-STI-2011-00005).

[18] Fawzy, Y. H. A., Soliman, F. A. S., Swidan, A., and Abdelmagid, A., 2008, "Characterization and Operation of PZT Ceramic Filters on Gamma-Radiation Environment," The Second All African IRPA Regional Radiation Protection Congress, Ismailia, Egypt, Apr. 22–26, p. 10.

[19] Yang, S. A., Kim, B. H., Lee, M. K., Lee, G. J., Lee, N. H., and Bu, S. D., 2014, "Gamma-Ray Irradiation Effects on Electrical Properties of Ferroelectric $PbTiO_3$ and Pb (Zr 0.52 Ti 0.48) O_3 Thin Films," Thin Solid Films, **562**, pp. 185–189.

[20] Augereau, F. P., Ferrandis, J. Y., Villard, J. F., Fourmentel, D., Dierckx, M., and Wagemans, J., 2008, "Effect of Intense Neutron Dose Radiation on Piezoceramics," J. Acoust. Soc. Am., **123**(5), p. 3928.

[21] Kundzins, K., Zauls, V., Kundzins, M., Sternberg, A., Čakare, L., Bittner, R., Humer, K., and Weber, H. W., 2001, "Neutron Irradiation Effects on Sol-Gel PZT Thin Films," Ferroelectrics, **258**(1), pp. 285–290.

[22] Sinclair, A. N., and Chertov, A. M., 2015, "Radiation Endurance of Piezoelectric Ultrasonic Transducers–A Review," Ultrasonics, **57**, pp. 1–10.

[23] Parks, D., and Tittmann, B., 2014, "Radiation Tolerance of Piezoelectric Bulk Single-Crystal Aluminum Nitride," IEEE Trans. Ultrason., Ferroelectr., Freq. Control, **61**(7), pp. 1216–1222.

[24] Kulikov, D., and Trushin, Y., 2004, "Theoretical Study of Ferroelectric Properties Degradation in Perovskite Ferroelectrics and Anti-Ferroelectrics Under Neutron Irradiation," Ferroelectrics, **308**(1), pp. 5–16.

[25] Giurgiutiu, V., Postolache, C., and Tudose, M., 2016, "Radiation, Temperature, and Vacuum Effects on Piezoelectric Wafer Active Sensors," Smart Mater. Struct., **25**(3), p. 035024.

[26] Zagrai, A. N., 2002, "Piezoelectric-Wafer Active Sensor Electro-Mechanical Impedance Structural Health Monitoring," Doctoral dissertation, University of South Carolina, Columbia, SC.

[27] Haider, M. F., Giurgiutiu, V., Lin, B., and Yu, L., 2017, "Irreversibility Effects in Piezoelectric Wafer Active Sensors After Exposure to High Temperature," Smart Mater. Struct., **26**(9), p. 095019.

[28] Kamas, T., Poddar, B., Lin, B., and Yu, L. L., 2015, "Assessment of Temperature Effect in Structural Health Monitoring With Piezoelectric Wafer Active Sensors," Smart Struct. Syst., **16**(5), pp. 835–851.

[29] Park, G., Kabeya, K., Cudney, H. H., and Inman, D. J., 1999, "Impedance-Based Structural Health Monitoring for Temperature Varying Applications," JSME Int. J. Ser. A, **42**(2), pp. 249–258.

[30] Haider, M. F., Lin, B., Yu, L., and Giurgiutiu, V., 2017, "Sensing Capabilities of Piezoelectric Wafer Active Sensors in Extreme Nuclear Environment," Nondestructive Characterization and Monitoring of Advanced Materials, Aerospace, and Civil Infrastructure, Vol. 10169, p. 101691Z.

[31] Sun, X., Lin, B., Bao, J., Giurgiutiu, V., Knight, T., Lam, P. S., and Yu, L., 2015, "Developing a Structural Health Monitoring System for Nuclear Dry Cask Storage Canister," SPIE Smart Structures and Materials, Nondestructive Evaluation and Health Monitoring, p. 94390N.

[32] Xu, F., Trolier-McKinstry, S., Ren, W., Xu, B., Xie, Z. L., and Hemker, K. J., 2001, "Domain Wall Motion and Its Contribution to the Dielectric and Piezoelectric Properties of Lead Zirconate Titanate Films," J. Appl. Phys., **89**(2), pp. 1336–1348.
[33] Kamel, T. M., and de With, G., 2008, "Grain Size Effect on the Poling of Soft Pb $(Zr, Ti)O_3$ Ferroelectric Ceramics," J. Eur. Ceram. Soc., **28**(4), pp. 851–861.
[34] Herbiet, R., Robels, U., Dederichs, H., and Arlt, G., 1989, "Domain Wall and Volume Contributions to Material Properties of PZT Ceramics," Ferroelectrics, **98**(1), pp. 107–121.
[35] Zhang, Q. M., Wang, H., Kim, N., and Cross, L. E., 1994, "Direct Evaluation of Domain-Wall and Intrinsic Contributions to the Dielectric and Piezoelectric Response and Their Temperature Dependence on Lead Zirconate-Titanate Ceramics," J. Appl. Phys., **75**(1), pp. 454–459.
[36] Jaffe, B., Cook, W. R., Jr., and Jaffe, H., 1971, *Piezoelectric Ceramics*, Academic Press, New York.
[37] Haider, M. F., Lin, B., Yu, L., and Giurgiutiu, V., 2016, "Characterization of Piezo Electric Wafer Active Sensors After Exposure to High Temperature," Pressure Vessels and Piping Conference, 37.
[38] Lin, B., Mendez-Torres, A. E., Gresil, M., and Giurgiutiu, V., 2012, "Structural Health Monitoring With Piezoelectric Wafer Active Sensors Exposed to Irradiation Effects," ASME Paper No. PVP2012-78848.
[39] Anderson, M., Zagrai, A. N., Daniel, J. D., Westpfahl, D. J., and Henneke, D., 2018, "Investigating Effect of Space Radiation Environment on Piezoelectric Sensors: Cobalt-60 Irradiation Experiment," J. Nondestr. Eval., Diagn. Prognostics Eng. Syst., **1**(1), p. 011007.
[40] O'Keefe, M., and Navrotsky, A., 1981, *Structure and Bonding in Crystals*, Academic Press, New York.
[41] Glidewell, C., 1975, "Some Chemical and Structural Consequences of Non-Bonded Interactions," Inorg. Chim. Acta, **12**(1), pp. 219–227.
[42] Haider, M. F., Mei, H., Lin, B., Yu, L., Giurgiutiu, V., Lam, P. S., and Verst, C., 2018, "Piezoelectric Wafer Active Sensors Under Gamma Radiation Exposure Toward Applications for Structural Health Monitoring of Nuclear Dry Cask Storage Systems," *Nondestructive Characterization and Monitoring of Advanced Materials, Aerospace, Civil Infrastructure, and Transportation XII*, Vol. 10599, International Society for Optics and Photonics, Denver, CO, p. 105992F.